PERGAMON

International Journal of Heat and Mass Transfer 42 (1999) 1141–1146

International Journal of HEAT and MASS TRANSFER

Technical Note
Optimization of inlet concentration profile for uniform deposition in a cylindrical chemical vapor deposition chamber

W. K. Cho, D. H. Choi*, M.-U. Kim

Department of Mechanical Engineering, Korea Advanced Institute of Science and Technology, Taejon 305-701, Korea

Received 4 July 1997; in final form 3 January 1998

1. Introduction

CVD (chemical vapor deposition) is a process which grows a thin film on a substrate, and can be applied to producing many important engineering devices such as microelectronic circuits, optical and magnetic recording media and high performance cutting/grinding tools [1]. The thickness of the thin film ranges from a few nm to tens of μm according to the objective of a product. One of the most important measures of quality of this thin film is 'uniformity of the thickness' and is crucial to the performance characteristics: device behavior, optical reaction, etc.

To attain uniform growth rate, various attempts have been made and reported in the literature. Controlling the flow path of the reactant gas can be effective by either altering the chamber shape or setting up baffles inside the chamber [2]. Making the susceptor rotate [3–5] can also improve the growth rate and its uniformity as the centrifugal force enhances the inflow of the new reactant gas by throwing the used gas outward.

Although the aforementioned studies can be useful in designing an efficient CVD chamber, they are mostly qualitative and very little effort has been devoted to the optimizing of the chamber shape or operating conditions. Optimization of the key parameters is a very complex problem as these variables are intricately related and thus cannot be controlled independently. As a first step toward this goal, we devised an optimization procedure to determine the inlet concentration distribution of the reactant gas, that results in the most uniform growth rate, and carried out an analysis to find an optimal concentration profile at the inlet for various flow rates. This is a relatively simple case since the concentration field is passive to the flow and temperature fields. The task, however, is by no means trivial as shall be seen later. The optimized profile may or may not be of the shape that can be easily produced. It is proper to mention here that the focus of the paper is how to obtain the optimal profile rather than discussing its economic feasibility. The procedure, if found successful, can serve as the basis for more complex and general optimization problems, such as the shape optimization, in the future.

2. Analysis procedure

The chamber of cylindrical shape shown in Fig. 1 is considered in the present study. The susceptor of radius r_s, on which the wafer is placed, is a distance H away from the inlet of radius r_{in} at the top and the reactant gas is blown in through the inlet and goes out via the gap between the chamber wall and the susceptor. Since the flow is axisymmetric, the governing equations of continuity, momentum and concentration in (r, x) coordinates may be written as:

$$\frac{1}{r}\frac{\partial}{\partial r}(rv_r)+\frac{\partial}{\partial x}(v_x)=0 \tag{1}$$

$$(V\cdot\nabla)v_r=-\frac{\partial p}{\partial r}+\frac{1}{Re}\left(\nabla^2 v_r-\frac{v_r}{r^2}\right) \tag{2}$$

$$(V\cdot\nabla)v_x=-\frac{\partial p}{\partial x}+\frac{1}{Re}(\nabla^2 v_x) \tag{3}$$

$$(V\cdot\nabla)C=\frac{1}{Re\cdot Sc}(\nabla^2 C) \tag{4}$$

where (v_r, v_x) are velocity components in (r, x) directions, respectively, p the total hydrostatic pressure, and C the

* Corresponding author. Tel: 00 82 42 869 3018; fax: 00 82 42 869 3210; e-mail: dhchoi@hanbit.kaist.ac.kr

PII: S0017–9310(98)00176–8

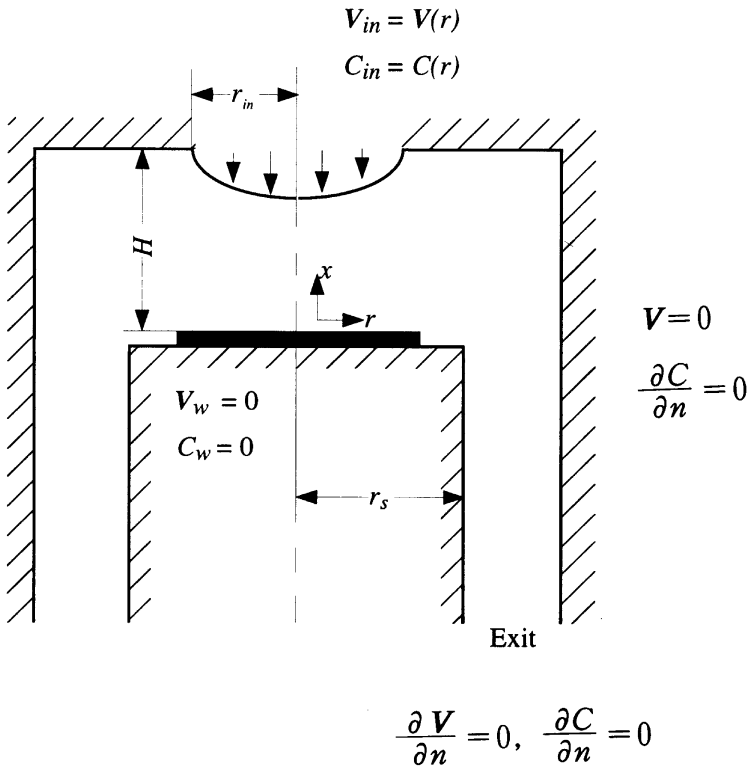

Fig. 1. Schematic of a vertical reactor.

concentration. These equations have been made dimensionless by using the mean inlet velocity v_{in}, the reference reactant gas concentration C_{ref} and the susceptor radius r_s. The dimensionless parameters Re $(= v_{in} r_s/v)$ and Sc $(= v/D)$ are Reynolds number and Schmidt number, where v and D denote the kinematic viscosity and the diffusivity, respectively. Note that the concentration equation (4) remains unchanged by the normalization using C_{ref} because of its linearity. Mathematically C_{ref} may take any value; however, in conjunction with equation (9) discussed later, it is linked to the deposition rate and should be fixed accordingly. Since the analysis is valid for any deposition rate, we treat it as an undetermined free parameter in the present study. It needs to be mentioned here that when the temperature variation is so large that the free-convection effects are not negligible, the system should include the energy equation as well as a buoyancy term in the momentum equation. The present procedure can be readily extended to solve such cases without much modification.

For the computational domain that extends from the inlet to the exit in one azimuthal plane (see Fig. 1), the following boundary conditions appear to simulate the real situation best:

Inlet (given)

$$v_x = 2((r/r_{in})^2 - 1), \quad v_r = 0$$
$$C = C(r) \tag{5}$$

Exit

$$\frac{\partial v_r}{\partial x} = \frac{\partial v_x}{\partial x} = \frac{\partial p}{\partial x} = \frac{\partial C}{\partial x} = 0 \tag{6}$$

Axis (symmetry)

$$\frac{\partial v_x}{\partial r} = \frac{\partial p}{\partial r} = \frac{\partial C}{\partial r} = 0, \quad v_r = 0 \tag{7}$$

Solid surface

$$v_r = v_x = 0, \quad \frac{\partial p}{\partial n} = 0$$
$$C = 0 \quad \text{(wafer surface)}$$
$$\frac{\partial C}{\partial n} = 0 \quad \text{(other surface)} \tag{8}$$

The parabolic inlet-velocity profile is arbitrary and may be given a different shape. The vanishing concentration at the wafer surface is the result of the deposition process that accompanies the chemical reaction. Also, since the amount of mass deposition compared with the flow rate

is negligible, the mass-depletion effects are not considered in the present study.

On a nonstaggered grid, the equations (1)–(4), subject to the boundary conditions (5)–(8), are solved by using the SIMPLE algorithm of Patankar [6]. The diffusive derivatives in the equations are discretized by the central differencing while the convective derivatives are done by the upwind differencing. The momentum interpolation scheme of Rhie and Chow [7] has been incorporated in the procedure to avoid the occurrence of the unrealistic checker-board pressure pattern. The process is iterative and the solution is considered converged when the following criterion is met:

$$\max\left[\sum_{i=1}|\mathrm{Res}(\phi_i^k)|\right] \leqslant 10^{-4}$$

where $|\mathrm{Res}(\phi_i^k)|$ is the absolute value of residual of kth equation at ith control volume.

3. Optimization technique

What we wish to accomplish here is to make the deposition rate as uniform as possible by controlling the inlet concentration distribution. Noting that the deposition rate is proportional to the normal concentration gradient on the wafer surface, the cost functional representing the area-weighted square error that needs to be minimized may be defined as

$$E = \int_{r=0}^{r=0.8} (\partial C/\partial x|_{x=0} - 1.0)^2 r\,\mathrm{d}r \tag{9}$$

The subtractive constant, 1.0, is interpreted as an average concentration gradient and its arbitrariness can be justified as the constant multiple is buried in the free parameter C_{ref} described earlier. This approximation (9) is valid if the reactant gas moves with the working fluid and the reaction occurs instantly as have been assumed in most other analyses. Since the concentration equation is decoupled from the momentum equations, the minimization process can be pursued after the flow field has been determined.

We conveniently excluded the corner point where the integrand becomes unbounded by choosing the upper limit of the integration (9) to be less than 1. The value of 0.8 is arbitrary and a larger value may be taken instead. However, pushing it close to 1 is neither practical nor meaningful as the integral will be dominated by the outer region where $\partial C/\partial x$ cannot be kept uniform anyway. Besides, this is not a severe constraint as the susceptor is always larger than the wafer size in a real situation to avoid the obvious irregular deposition close to the corner point.

The inlet concentration profile may be expressed as a linear combination of basis functions $\phi_k(r)$ as

$$C_{\mathrm{in}}(r) = \sum_{k=1}^{N} a_k \phi_k(r) \tag{10}$$

where N is the number of functions used. Since $C_{\mathrm{in}}(r)$ is symmetric about r, we chose the Chebyshev polynominal of even degree as the basis function in view of its orthogonality and excellent properties of approximating functions.

For each inlet concentration $\phi_k(r)$, there is a corresponding concentration gradient distribution $\psi_k(r)$ $(= \partial C(r)/\partial x)$ along the wafer surface. This is obtained as part of the solution using the procedure described in the previous section. The linearity of the system allows us to write the concentration gradient associated with the inlet condition (10) as

$$\partial C/\partial x|_{x=0} = \sum_{k=1}^{N} a_k \psi_k(r) \tag{11}$$

The task now is to find a set of coefficients a_k that minimizes the integral (9).

The optimization process is carried out by using the local random search technique in Vanderplaats [8]. The basic concept is to locate the point that minimizes the cost functional in a randomly generated search direction. A new minimum point is obtained in a subsequently generated random search direction; the process is continued until convergence.

4. Results and discussions

The code was first verified against the earlier numerical results [9] for flow of similar characteristics, circular pipe with sudden contraction, by confirming that the axial velocity profiles at various cross-sections are in good agreement: the discrepancy in the momentum and displacement thickness at stations right before and after the contraction is less than 2%. The first set of calculations of present interest was made for $H = r_{\mathrm{in}} = r_{\mathrm{s}}/2$ and the gap between the susceptor and the chamber wall of $r_{\mathrm{s}}/2$. The exit boundary of the computational domain is placed at a distance $2.5r_{\mathrm{s}}$ downstream of the susceptor face. The length of the gap region amounts to 5 times the gap width and was found to be sufficiently long to obtain the domain-independent solution in the main region. With H_2 and $(CH_3)_3Ga$ as working fluid and reactant gas, the Schmidt number comes out as 2.33 since $\upsilon = 7 \times 10^{-3}(\mathrm{m}^2\ \mathrm{s}^{-1})$ and $D = 3 \times 10^{-3}(\mathrm{m}^2\ \mathrm{s}^{-1})$, owing to the formulas in Fortiadis et al. [2] at 900 K and 0.1 atm. A 135×90 nonuniformly distributed grid, which is finer near the inlet and the susceptor edge, was selected after much grid-dependency test.

The flow and concentration fields for three different Reynolds numbers, 1, 10, and 100 are presented in Fig. 2. The streamline patterns shown in Fig. 2(a) look all similar except that the streamlines are packed closer to

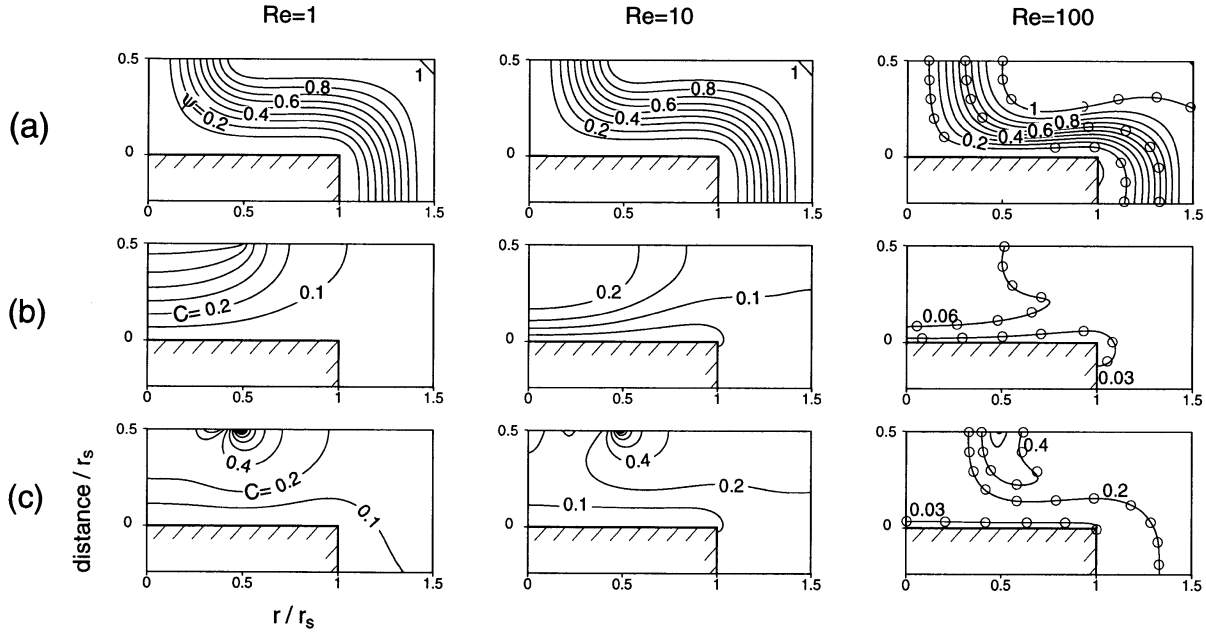

Fig. 2. Flow and concentration fields for various Reynolds numbers (—: 135×90, ○: 90×60): (a) streamlines, (b) unoptimized concentration fields, (c) optimized concentration fields.

the wafer surface and the recirculating region gets larger with increasing Re. Figure 2(b), (c) exhibit the concentration distributions with and without optimization: Fig. 2(b), which corresponds to the uniform (i.e., unoptimized) inlet concentration, shows that the equi-concentration lines near the wafer surface deviate much from the parallel-to-the-surface position. This results in non-uniform normal concentration-gradient $\partial C/\partial x$ distribution along the wafer surface and, consequently, the non-uniform deposition rate. On the other hand, those obtained from the optimized inlet distribution, Fig. 2(c), become nearly parallel to the wafer surface. The symbol represents the solution obtained with a coarser grid (90×60) and the close agreement indicates that the present grid is fine enough to resolve the flow field.

The improvement is better depicted in Fig. 3 that presents the optimized concentration-gradient distributions for given degrees of inlet concentration profile—$n = 1$, 2, 3, and 4 denote inlet profile degree of 0, 2, 4, and 6 respectively. For all three Reynolds number cases, $n \geqslant 3$ gives as uniform a concentration gradient distribution as possible by controlling the inlet concentration. Further addition of higher-degree basis functions improves the results very little. This is very encouraging, in a practical standpoint, as it makes the optimization process and the desirable inlet profile relatively simple. Also it is useful to note that, for all cases, the concentration is lower at the center of the inlet.

The flow of $Re = 1$ is diffusion dominant and relatively little can be gained by controlling the inlet distribution as the fluid mixes quickly due to diffusion. As seen in Fig. 3(a), despite a substantial change in the inlet profiles between $n = 3$ and 4, the associated concentration gradients appear to be indiscernible. Conversely, when $Re = 100$, the convection is significant and the change in the inlet profile is directly reflected on the normal gradient on the wafer surface. The improvement is fairly rapid and $n = 3$ gives perfectly uniform results. How the results improve as the number of basis functions increases is shown in Fig. 4, which plots the variation of the cost functional versus the number of functions. As has been mentioned, the improvement is limited when $Re = 1$, fast and substantial for $Re = 100$, and gradual but steady when $Re = 10$.

Similar characterization can be made when the distance to the wafer surface from the inlet is varied for a fixed Reynolds number. As the distance becomes larger, the mixing due to diffusion dominates and the control of inlet profile has a smaller effect on the deposition uniformity whereas when the wafer is closer to the inlet, the reactant gas reaches the surface without much mixing and the optimization is proved to be effective. These have

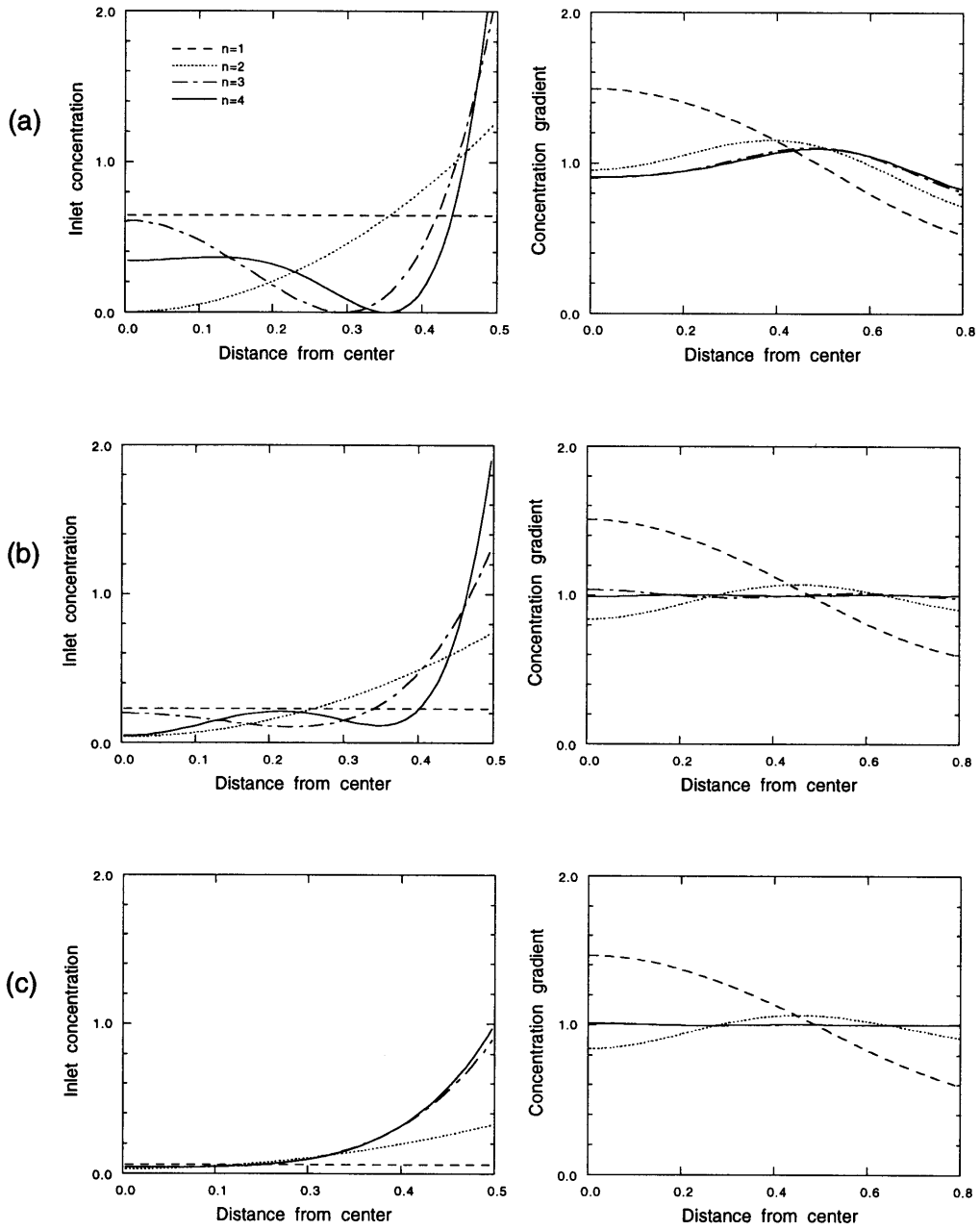

Fig. 3. Inlet concentration profiles and corresponding concentration-gradient distributions on wafer surface: (a) $Re = 1$, (b) $Re = 10$, (c) $Re = 100$.

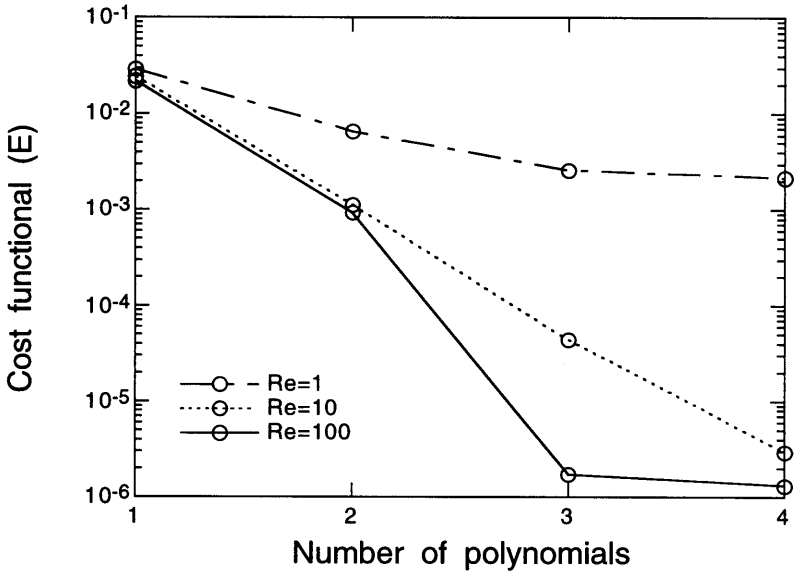

Fig. 4. Cost functional vs number of basis functions.

been confirmed by a series of calculations, however, the results are not presented here for brevity.

Acknowledgement

Support of this research by Samsung Electronics Co. is gratefully acknowledged.

References

[1] K.F. Jensen, Flow phenomena in chemical vapor deposition of thin films, Ann. Rev. Fluid Mech. 23 (1991) 197–232.
[2] D.I. Fortiadis, S. Kieda, K.F. Jensen, Transport phenomena in vertical reactors for metalorganic vapor phase epitaxy, Journal of Crystal Growth 102 (1990) 441–470.
[3] G. Evans, R. Greif, A numerical model of the flow and heat transfer in a rotating disk chemical vapor deposition reactor, Journal of Heat Transfer 109 (1987) 928–935.
[4] S. Patnaik, R.A. Brown, C.A. Wang, Hydrodynamic dispersion in rotating-disk OMVPE reactors: numerical simulation and experimental measurements, Journal of Crystal Growth 96 (1989) 153–174.
[5] W.S. Winters, G.H. Evans, R. Greif, Mixed binary convection in rotating disk chemical vapor deposition reactor, International Journal of Heat and Mass Transfer 40 (3) (1997) 737–744.
[6] S.V. Patankar, Numerical Heat Transfer and Fluid Flow, McGraw-Hill, 1980.
[7] C.M. Rhie, W.L. Chow, A numerical study of the turbulent flows past an isolated airfoil with trailing edge separation, AIAA Journal 21 (1983) 1525–1532.
[8] G.N. Vanderplaats, Numerical Optimization Techniques for Engineering Design, McGraw-Hill, 1984, pp. 153–155.
[9] M. Peric, A finite volume method for the prediction of three-dimensional fluid flow in complex ducts, PhD thesis, University of London, 1985, pp. 198–207.